ACS Macro Letters

Letter

pubs.acs.org/macroletters

# Self-Assembly of Monotethered Single-Chain Nanoparticle Shape Amphiphiles

Jianguo Wen,[†] Liang Yuan,[‡] Yongfang Yang,[†] Li Liu,*[,§] and Hanying Zhao*[,‡]

Key Laboratory of Functional Polymer Materials, Ministry of Education, [‡]Department of Chemistry, [§]Institute of Polymer Chemistry, Nankai University, Tianjin 300071, China

[†]Institute of Polymer Science and Engineering, Hebei University of Technology, Tianjin 300130, China

Supporting Information

**ABSTRACT:** Shape amphiphiles with distinct shapes and amphiphilic properties can be used as fundamental building blocks in the fabrication of novel structures and advanced materials. In this research synthesis and self-assembly of monotethered single-chain nanoparticle shape amphiphiles are reported. Poly(2-(dimethylamino)ethyl methacrylate)-*block*-polystyrene (PDMAEMA-*b*-PS) was synthesized by two-step reversible addition–fragmentation chain transfer (RAFT) polymerization. The PDMAEMA blocks were intramolecularly cross-linked by 1,4-diiodobutane (DIB) at significantly low concentrations, and PS-tethered PDMAEMA single-chain nanoparticles were prepared. Gel permeation chromatograph, $^1$H NMR and transmission electron microscopy results all indicated successful synthesis of the structures. The controlled self-assembly of the shape amphiphiles in selective solvents was investigated. Depending on the size of the single-chain nanoparticles, the shape amphiphiles self-assemble into strawberry-like micelles, a structure with single-chain nanoparticles in the corona and PS in the core, or vesicles in aqueous solutions. Similar to the self-assembled structures in aqueous solution, the morphology of the aggregates in methanol changes from micellar structure to vesicular structure with the decrease of the PDMAEMA single-chain nanoparticles size. In cyclohexane, the shape amphiphiles self-assemble into bunchy micelles with single-chain nanoparticles in the cores and linear PS in the coronae.

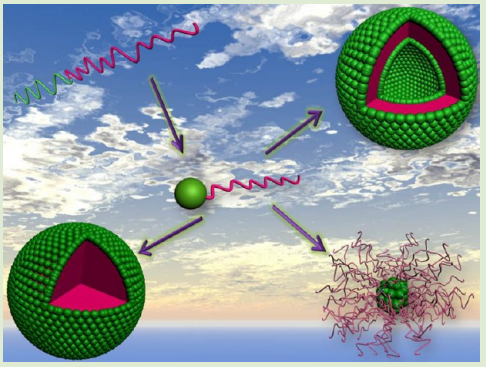

It is well-known that small-molecule surfactants, amphiphilic block copolymers and graft copolymers are able to self-assemble into micelles in aqueous phases.[1] For example, in amphiphilic block copolymer assemblies, the hydrophobic blocks form the cores of the structures, whereas the hydrophilic blocks form the coronae. Self-assembly of block copolymers has been studied both from theoretical and experimental points of view due to the wide applications of the self-assembled structures.[2] In this decade, with the development of nanoscience and nanotechnology many new "nanoobjects" and particles are produced, which can be used as new building blocks in the fabrication of novel structures by self-assembly approach. Shape amphiphiles are a type of building blocks with distinct shapes and amphiphilic properties and are able to spontaneously organize into ordered arrangements.[3] Patchy particles prepared by decorating the specific surface of the particles with "sticky patches" and tethered nanoparticles synthesized by attaching polymer chains to the nanoparticles are two typical classes of shape amphiphiles.[4]

In 1997, Marques published a theoretical study on the micellar aggregation of a shape amphiphile with an insoluble solid bead and a soluble long tadpole tail.[5] His results indicate that the tadpole-like molecules are able to self-assemble into micelles. The core of a micelle is composed of solid beads and has a porous structure. Recently, synthesis and self-assembly of shape amphiphiles based on polymer chain tethered polyhedral oligomeric silsesquioxanes (POSS) and polyoxometalate (POM) were reported.[6,7] The self-assembled morphology can be tuned from vesicles to wormlike cylinders and to spherical micelles.

In this decade, intramolecular cross-linking of linear polymer chains has been an efficient route to the synthesis of structurally well-defined nanoparticles.[8,9] In a dilute polymer solution with a concentration below the overlap concentration, the dimensions of individual polymer chains are smaller than the average distance between the two chains and the polymer coils in solution simply do not have contact with each other, cross-linking reactions at such low concentrations will result in intrachain cross-linkings.[9] After intramolecular cross-linking reaction, a linear polymer chain presents a coil-to-globule transition and a single-chain nanoparticle is prepared. Besides linear polymer chains, intramolecular cross-linkings of core–shell brush polymers were also reported.[10,11]

Most previous researches were focused on the synthesis of single-chain nanoparticles by different methods; however, the use of single-chain nanoparticles as elementary building blocks

**Received:** December 7, 2012
**Accepted:** January 8, 2013
**Published:** January 11, 2013

   dx.doi.org/10.1021/mz300636x | *ACS Macro Lett.* 2013, 2, 100–106

in the bottom-up self-assembly approach has not been touched. Herein, we report the synthesis and self-assembly of polymer chain tethered single-chain nanoparticle amphiphiles in selective solvents. In such a molecular structure, there is only one hydrophobic polymer chain tethered to a single-chain nanoparticle, so we call this type of structure monotethered single-chain nanoparticle shape amphiphiles. Poly(2-(dimethylamino)ethyl methacrylate)-*block*-polystyrene (PDMAEMA-*b*-PS) was synthesized by reversible addition–fragmentation chain transfer (RAFT) polymerization. The PDMAEMA blocks were partly cross-linked by 1,4-diiodobutane (DIB) at significantly low concentrations, and monotethered single-chain nanoparticle shape amphiphiles were prepared. A shape amphiphile molecule is composed of a positively charged PDMAEMA single-chain nanoparticle and a PS chain tethered to the nanoparticle (scheme 1). The controlled self-assemblies of the well-defined shape amphiphiles in selective solvents were investigated in this research.

**Scheme 1. Outline for the Synthesis of Shape Amphiphiles with Poly(2-(dimethylamino)ethyl methacrylate) (PDMAEMA) Single-Chain Nanoparticles and Polystyrene (PS) Tails by Two-Step RAFT Polymerization and Intramolecular Cross-Linking Reaction**

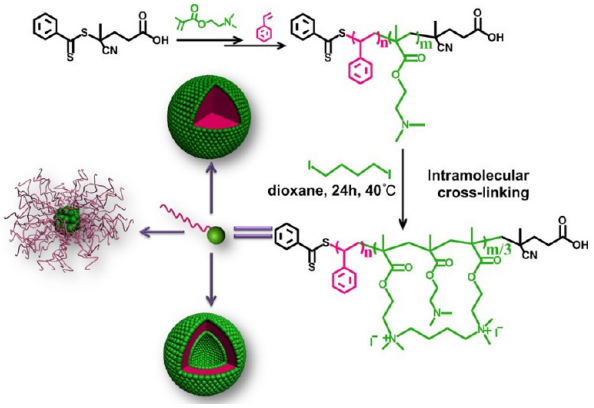


The average size of the single-chain nanoparticles is dependent on the molecular weight of the precursor polymer, and the size distribution of the nanoparticles is dependent on the polydispersity. To prepare well-defined single-chain nanoparticle-coil structures, linear diblock copolymers with well-defined structures and low molecular weight distributions are required. In this research two PDMAEMA-*b*-PS linear diblock copolymers with different compositions were synthesized by two-step RAFT polymerizations (Scheme 1). $^1$H NMR result shows that the average repeating unit numbers of PDMAEMA and PS in the two block copolymers are 74, 297 and 15, 151. In this paper, the two precursor linear block copolymers are denominated as PDMAEMA$_{74}$-*b*-PS$_{297}$ and PDMAEMA$_{15}$-*b*-PS$_{151}$, respectively. Based on size exclusion chromatography (SEC) results, the apparent molecular weights ($M_n$) and the polydispersities of the two diblock copolymers are 33.4 K, 1.20, and 17.4 K, 1.17.

The quaternization reactions were widely used in the preparation of cross-linked structures.[12] In this research, the quaternization reaction between PDMAEMA and DIB was used in the preparation of single-chain nanoparticles. In order to avoid intermolecular cross-linking and promote efficient formation of single-chain nanoparticles, intramolecular cross-linking of PDMAEMA-*b*-PS was conducted in 1,4-dioxane at a very low concentration by adding dropwise DIB into the polymer solution. The degree of cross-linking was controlled by controlling the amount of DIB used in the reaction. With the intramolecular cross-linking reaction, PDMAEMA blocks collapse forming single-chain nanoparticles, and quaternary ammonium salts are produced on the nanoparticles. In this paper, the single-chain nanoparticle-coil structures are referred to as NP$_n$-PDMAEMA-*b*-PS, where *n* represents the percentage of the quaternary ammonium salts in PDMAEMA block, which can be determined by the amount of iodine in the block coolymer.

When unimolecular particles are formed by intramolecular cross-linking of linear polymer chains, a reduction in hydrodynamic radius, as well as the average apparent molecular weight, is observed due to the collapse of the linear polymer chains.[13] Part a in Figure 1 compares SEC traces for

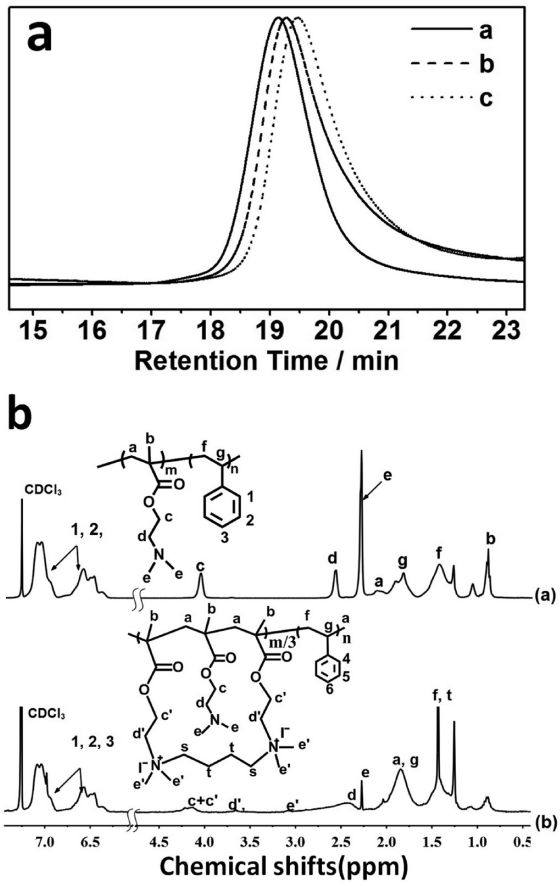


**Figure 1.** (a) SEC traces of PDMAEMA$_{74}$-*b*-PS$_{297}$ (curve a), NP$_{0.1}$-PDMAEMA$_{74}$-*b*-PS$_{297}$ (curve b), and NP$_{0.2}$-PDMAEMA$_{74}$-*b*-PS$_{297}$ (curve c); (b) $^1$H NMR spectra of PDMAEMA$_{74}$-*b*-PS$_{297}$ (spectrum a) and NP$_{0.2}$-PDMAEMA$_{74}$-*b*-PS$_{297}$ (spectrum b).

PDMAEMA$_{74}$-*b*-PS$_{297}$, NP$_{0.1}$-PDMAEMA$_{74}$-*b*-PS$_{297}$ and NP$_{0.2}$-PDMAEMA$_{74}$-*b*-PS$_{297}$. In comparison to the linear precursor block copolymer, the increase in the retention time suggests the decrease of the hydrodynamic volume of the block copolymer after intramolecular cross-linking of PDMAEMA blocks, and the formation of the single-chain nanoparticle-coil structures. The apparent number-average molecular weights of PDMAEMA$_{74}$-*b*-PS$_{297}$, NP$_{0.1}$-PDMAEMA$_{74}$-*b*-PS$_{297}$, and NP$_{0.2}$-PDMAEMA$_{74}$-*b*-PS$_{297}$, as determined by SEC are 33.4K, 27.4K, and


dx.doi.org/10.1021/mz300636x | *ACS Macro Lett.* 2013, 2, 100–106

26.1K. A reduction in the apparent molecular weight demonstrates the intramolecular cross-linking of PDMAEMA blocks by DIB. The number-average molecular weights and polydispersities of the nanoparticle-coil structures and their precursors are summarized in Table S1 (Supporting Information). Figure 1b shows $^1$H NMR spectra of PDMAEMA$_{74}$-*b*-PS$_{297}$ and NP$_{0.2}$-PDMAEMA$_{74}$-*b*-PS$_{297}$. In the spectrum of PDMAEMA$_{74}$-*b*-PS$_{297}$, the peaks at 7.14 and 6.69 ppm represent phenyl protons on styrene repeating units, and the peaks at 4.09 and 2.62 ppm are assigned to the methylene protons neighboring ester group and nitrogen atom in DMAEMA repeating units, whereas the peak at 2.33 ppm is attributed to the methyl protons connecting to the nitrogen atom. In comparison to the linear block copolymer, the intensities of the peaks corresponding to the protons on PDMAEMA blocks at 4.09, 2.62, and 2.33 ppm decrease significantly after cross-linking reaction, which can be rationalized by the cross-lonking of the PDMAEMA blocks limiting the rotational and diffusional mobility of the protons on the repeating units. It is worthy to note that strong signals corresponding to the phenyl protons are still observed even after intramolecular cross-linking reaction, which indicates that PS blocks are still solvated after the intramolecular cross-linking reaction.

By controlling the molecular weight of the linear precursor polymer and the cross-linking degree, single-chain nanoparticles in the range from a couple of nanometers to 20 nm can be synthesized. Transmission electron microscopy (TEM) is a powerful tool in the study of materials in this size range, and TEM measurement is able to provide direct evidence to the formation of single-chain nanoparticles.[14] In this research monotethered single-chain nanoparticle shape amphiphiles were further characterized by TEM. Figure 2a,b shows two TEM images of NP$_{0.1}$-PDMAEMA$_{74}$-*b*-PS$_{297}$ and NP$_{0.2}$-PDMAEMA$_{74}$-*b*-PS$_{297}$ prepared by casting from THF solutions. The single-chain nanoparticles are cross-linked by DIB, and iodine in the nanoparticles enhances the contrast between the nanoparticles and the background, so no staining is necessary. In the TEM images, narrowly dispersed spherical nanoparticles are observed and the average size of NP$_{0.1}$-PDMAEMA$_{74}$-*b*-PS$_{297}$ and NP$_{0.2}$-PDMAEMA$_{74}$-*b*-PS$_{297}$ are 4.4 and 4.0 nm, respectively. Figure 2c shows DLS curves of NP$_{0.1}$-PDMAEMA$_{74}$-*b*-PS$_{297}$ and NP$_{0.2}$-PDMAEMA$_{74}$-*b*-PS$_{297}$ in THF. The average hydrodynamic diameters of the two structures are 6.0 and 4.8 nm, respectively. Both TEM and DLS results suggest that the average size of the structures decreases with the increase of the amount of DIB used in the cross-linking reaction. Figure 2d shows a TEM image of NP$_{0.34}$-PDMAEMA$_{15}$-*b*-PS$_{151}$. The average size of the nanoparticles is about 2 nm. Because the precursor diblock copolymer PDMAEMA$_{15}$-*b*-PS$_{151}$ has shorter PDMAEMA blocks, the size of NP$_{0.34}$-PDMAEMA$_{15}$-*b*-PS$_{151}$ is smaller than the single-chain nanoparticles formed by PDMAEMA$_{74}$-*b*-PS$_{297}$ at two different cross-linking degrees. Figure 2e represents a tapping mode AFM image of NP$_{0.1}$-PDMAEMA$_{74}$-*b*-PS$_{297}$ dispersed on mica surface from dilute solution. Spherical single-chain nanoparticles can be found in the image. The average size of the nanoparticles is about 10 nm, which is slightly bigger than TEM result (Figure 2a). The difference can be explained by the strong interaction between the positively charged nanoparticles and the polar mica substrate, and the deformation of the structures.

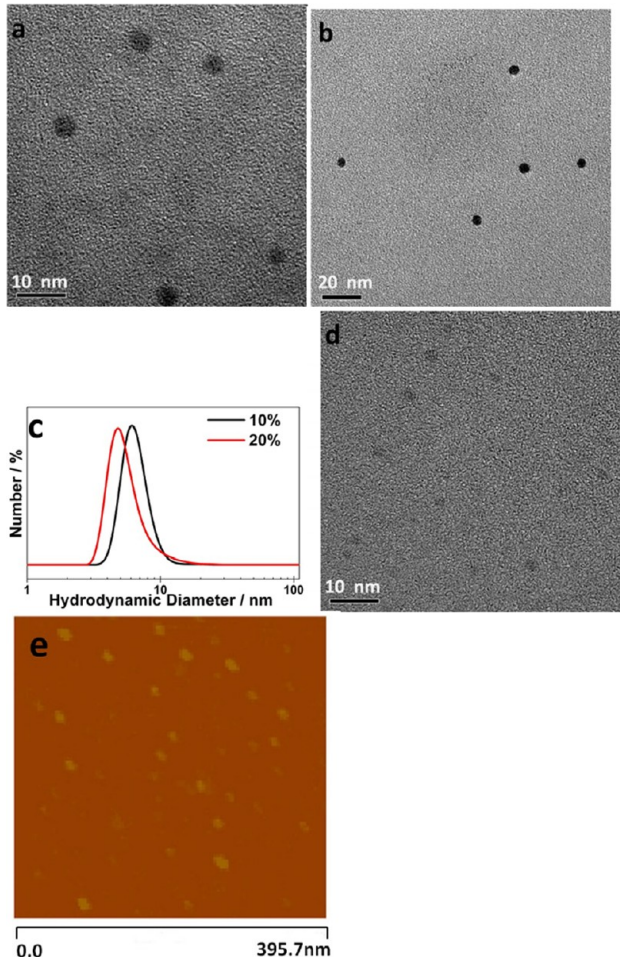


**Figure 2.** TEM images of (a) NP$_{0.1}$-PDMAEMA$_{74}$-*b*-PS$_{297}$, (b) NP$_{0.2}$-PDMAEMA$_{74}$-*b*-PS$_{297}$, and (d) NP$_{0.34}$-PDMAEMA$_{15}$-*b*-PS$_{151}$ prepared by casting from THF solutions; (c) dynamic light scattering curves of NP$_{0.1}$-PDMAEMA$_{74}$-*b*-PS$_{297}$ and NP$_{0.2}$-PDMAEMA$_{74}$-*b*-PS$_{297}$, and (e) tapping mode AFM micrograph of NP$_{0.1}$-PDMAEMA$_{74}$-*b*-PS$_{297}$ adsorbed on the surface of mica.

A shape amphiphile molecule synthesized in this research has one hydrophilic nanoparticle head and one hydrophobic PS tail, so it is expected that the well-defined shape amphiphiles are able to self-assemble into ordered structures in aqueous solutions. In order to study self-assemblies of the shape amphiphiles in aqueous media, polymers were dissolved in THF and 6-fold of water were added into the solutions at stirring, and colloidal solutions were obtained after dialysis of the solutions against water. Figure 3a,b represents TEM images of aggregates of NP$_{0.1}$-PDMAEMA$_{74}$-*b*-PS$_{297}$ observed at two different magnifications. At low magnification, spherical micelles in the size range from 17 to 50 nm are observed (Figure 3a). The average size of the micelles is about 30 nm. At high magnification single-chain nanoparticles on the surfaces of the micelles are observed (Figure 3b). The inset of Figure 3a shows a DLS curve of the micelles in aqueous solution. The average hydrodynamic diameter of the micelles is about 38 nm. In a self-assembly structure, PS chains collapse forming the core of a micelle and the hydrophilic single chain nanoparticles are in the corona to stabilize the micellar structure. Because the surfaces of the micelles are decorated by single-chain nanoparticles, we call them strawberry-like micelles. Figure 3c presents an AFM image of the micelles formed by NP$_{0.1}$-


dx.doi.org/10.1021/mz300636x | *ACS Macro Lett.* 2013, 2, 100−106

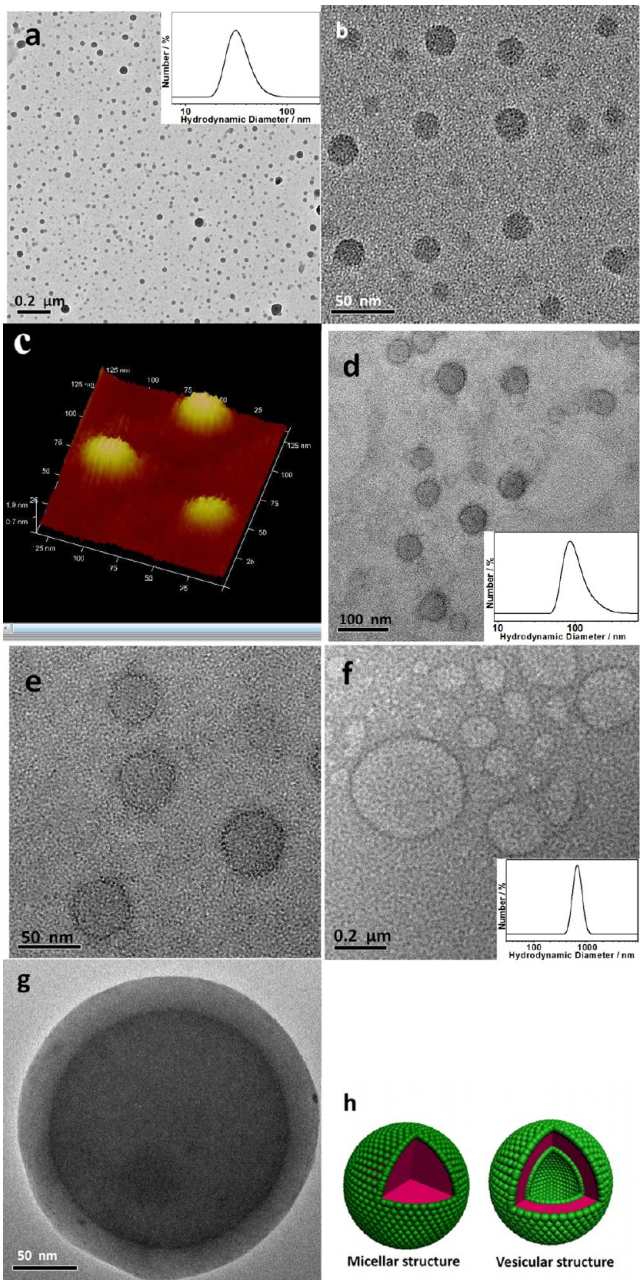


**Figure 3.** TEM images of self-assembly aggregates of $NP_{0.1}$-$PDMAEMA_{74}$-*b*-$PS_{297}$ (a, b), $NP_{0.2}$-$PDMAEMA_{74}$-*b*-$PS_{297}$ (d, e), and $NP_{0.34}$-$PDMAEMA_{15}$-*b*-$PS_{151}$ (f, g) in aqueous solutions, tapping mode AFM image of self-assembly aggregates of $NP_{0.1}$-$PDMAEMA_{74}$-*b*-$PS_{297}$ (c), and (h) cartoon pictures showing the details of the micellar structure and vesicular structure self-assembled by shape amphiphiles. The insets of parts a, d, and f are DLS curves of self-assembly structures in aqueous solutions.

$PDMAEMA_{74}$-*b*-$PS_{297}$. The average size of the micelles is about 40 nm, which is bigger than TEM result; however, the height of the structures is much smaller than their diameter. The bigger size and lower height of the aggregates indicate the strong interaction between the aggregates and the substrate surface, and the deformation of the structures. In the AFM image, the single-chain nanoparticles on the surfaces of the aggregates can be observed clearly, which demonstrate that the surfaces of the micelles are stabilized by positively charged single-chain nanoparticles.

Figure 3d,e shows two TEM images of micelles formed by $NP_{0.2}$-$PDMAEMA_{74}$-*b*-$PS_{297}$ in aqueous solutions. Based on the TEM result the average size of the micelles is about 50 nm. In a magnified TEM image single-chain nanoparticles in the coronae can be observed clearly (Figure 3e). The inset of Figure 3d shows a DLS curve of the micelles in aqueous solution. The average hydrodynamic diameter of the strawberry-like micelles is about 91 nm. When a dispersed particle moves through a liquid medium, a thin liquid layer adheres to its surface. Because of the influences of the liquid layer, the hydrodynamic diameter of the particles measured by DLS is bigger than the size determined by TEM. In aqueous solutions, the micellar structures are stabilized by the positively charged quaternary ammonium salts on the surface of the single chain nanoparticles, so the micelles are positively charged. The zeta potentials of the micelles formed by $NP_{0.1}$-$PDMAEMA_{74}$-*b*-$PS_{297}$ and $NP_{0.2}$-$PDMAEMA_{74}$-*b*-$PS_{297}$ are 7.2 and 17.5 mV, respectively. PDMAEMA is a pH-sensitive polymer in aqueous solution. At room temperature, PDMAEMA is water-soluble at low pH values, however, it precipitates from neutral or basic aqueous solution.[15] In this study, the micellar solution was controlled at neutral pH, so PDMAEMA chains inside the single-chain nanoparticles are kept at collapsed state, and the quaternized DMAEMA units located at the surface of single-chain nanoparticles stabilize the micellar structures. A scheme showing the details of a micellar structure is presented in Figure 3h.

Amphiphilic linear block copolymers are able to self-assemble into multiple morphologies in solution. Depending on the length of the hydrophilic block, the morphology can vary from spherical micelles, rods, and vesicles. For example, Eisenberg and co-worker synthesized polystyrene-*block*-poly(acrylic acid) (PS-*b*-PAA) with different PAA chain lengths and found that with decreasing PAA block lengths the morphology changes from spherical to rod-like, to vesicles, and to micrometer-size spheres.[16] To investigate the relationship between the morphology and the composition of the shape amphiphiles, self-assembly of $NP_{0.34}$-$PDMAEMA_{15}$-*b*-$PS_{151}$, a structure with smaller single-chain nanoparticles, was conducted in aqueous solution. A TEM image of self-assembly structures formed by $NP_{0.34}$-$PDMAEMA_{15}$-*b*-$PS_{151}$ in aqueous solution is shown in Figure 3f. In the image, the appearance of the dark rings in the self-assembly structures indicates the formation of the vesicles. To avoid unfavorable interaction with water, PS blocks in the tadpole-like macromolecules collapse forming the walls of vesicles, while the positively charged single chain nanoparticles distribute at the inner and outer surfaces to stabilize the structures. A scheme showing a vesicle structure is presented in Figure 3h. A magnified TEM image of a specific vesicular structure is shown in Figure 3g. Based on the TEM result, the thickness of the walls are determined to be about 20 to 25 nm. DLS curve of the self-assembly aggregates of $NP_{0.34}$-$PDMAEMA_{15}$-*b*-$PS_{151}$ is shown in the inset of Figure 3f. The hydrodynamic diameters of the structures are in the range from 200 to more than 1000 nm, which are much bigger than the micellar structures self-assembled by $NP_{0.1}$-$PDMAEMA_{74}$-*b*-$PS_{297}$ or $NP_{0.2}$-$PDMAEMA_{74}$-*b*-$PS_{297}$ in aqueous solutions. The significant changes in the morphology and sizes of the self-assembled structures are attributed to the polymer structures. The morphologies of amphiphilic linear block copolymers are governed by a balance of contributions to the free energy including the interfacial energy, the stretching of the core blocks and the repulsive interactions among the corona


dx.doi.org/10.1021/mz300636x | *ACS Macro Lett.* 2013, 2, 100−106

chains.[17] The morphology and size changes of the PS tethered PDMAEMA single-chain nanoparticles in solution are also driven by the change of the free energy. With the decreases in PDMAEMA block length and the hydrophilicity of the single chain nanoparticles, the free energy of the system increases, and the system minimizes the total interfacial area by forming vesicular structures and increasing their sizes.

In the preparation of PS tethered single-chain nanoparticles, the cross-linking degree is controlled at low level, and most DMAEMA repeating units are unquaternized. A question that arises from the previous studies is whether unquaternized PDMAEMA segments inside the single-chain nanoparticles can stabilize the self-assembled structures in solution. In order to answer this question, the self-assembly of the macromolecules in methanol is conducted, where methanol is a good solvent for PDMAEMA and a precipitant for PS. Figure S1 in Supporting Information part shows the change of optical transmittance versus volume percentage of methanol added into THF solution of $NP_{0.1}$-$PDMAEMA_{74}$-*b*-$PS_{297}$. As the polymer aggregates together, the turbidity of the solution increases, and the transmittance decreases. Our experimental result shows that when the volume percentage of methanol reaches 10%, the transmittance of the solution starts to decrease indicating the start of the self-assembly of the polymer, and when the volume percentage reaches 30%, the transmittance levels off. Figure 4a,b shows two TEM images of aggregates assembled by $NP_{0.1}$-$PDMAEMA_{74}$-*b*-$PS_{297}$ in methanol. Spherical micelles with an average size of 29 nm are formed by $NP_{0.1}$-$PDMAEMA_{74}$-*b*-$PS_{297}$ in methanol (Figure 4a). In a magnified TEM image, single-chain nanoparticles on the surfaces of the micelles can be observed (Figure 4b). DLS curve of the micelles in methanol is presented in the inset of Figure 4a. The average hydrodynamic diameter of the micelles is about 30 nm, which is very close to the size measured by TEM. Two TEM images of micelles formed by $NP_{0.2}$-$PDMAEMA_{74}$-*b*-$PS_{297}$ in methanol are shown in Figure 4c,d. Based on TEM results, the average size of the micelles is about 36 nm. A magnified TEM image of the micelles is shown in Figure 4d. In the image single-chain nanoparticles in the coronae of the micelles are observed, which indicate that the micellar structures are stabilized by solvated PDMAEMA entrapped inside the single-chain nanoparticles. DLS curve of the micelles is presented in the insert of Figure 4c. The hydrodynamic diameters of the micelles are in the range from 20 to 80 nm with an average value at about 38 nm. So our TEM and DLS results both demonstrate that the PDMAEMA segments inside the single-chain nanoparticles are also able to stabilize the micellar structures.

Figure 4e and f are two TEM images of aggregates of $NP_{0.34}$-$PDMAEMA_{15}$-*b*-$PS_{151}$ in methanol. In the TEM image, large spherical vesicles with sizes in the range from 100 to 500 nm are observed, which indicates that similar to the self-assembly of the macromolecules in aqueous solution, with decreases in PDMAEMA block length and the average size of the single-chain nanoparticles the morphology of the aggregates in methanol changes from micellar structure to vesicular structure. DLS curve of the vesicles is shown in the insert of Figure 4e, which indicates that the hydrodynamic diameter of the aggregates is in the range from 180 to 500 nm. A magnified TEM image of a specific vesicle is presented in Figure 4f. Based on the TEM image, the thickness of the wall is calculated to be about 14 nm.

In a previous paper, Marques reported a theoretical study on the micellization of macrosurfactants with a soluble long

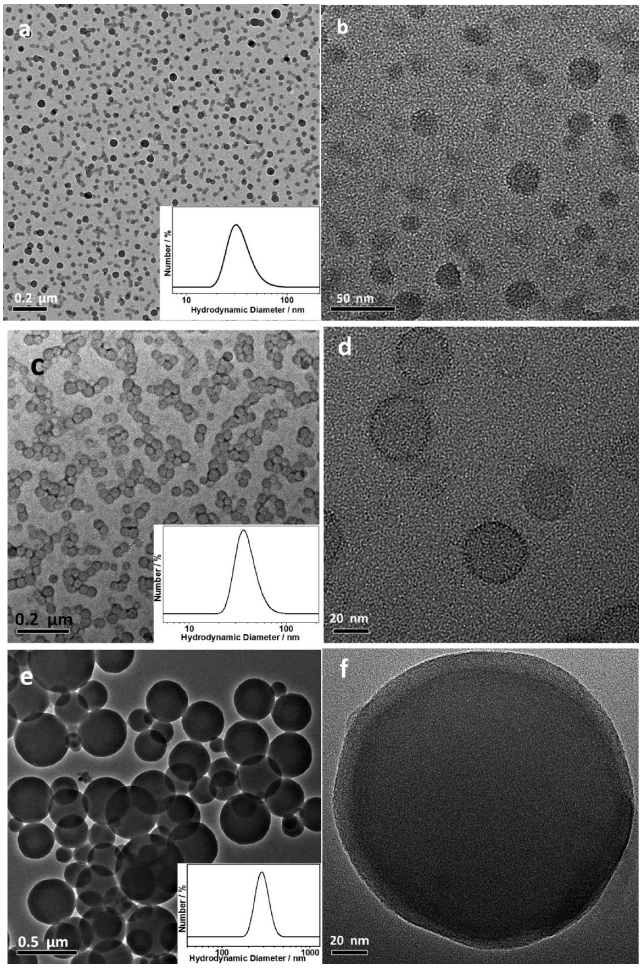


**Figure 4.** TEM images of self-assembly aggregates of $NP_{0.1}$-$PDMAEMA_{74}$-*b*-$PS_{297}$ (a, b), $NP_{0.2}$-$PDMAEMA_{74}$-*b*-$PS_{297}$ (c, d), and $NP_{0.34}$-$PDMAEMA_{15}$-*b*-$PS_{151}$ (e, f) in methanol solutions. The insets of parts a, c, and e are DLS curves of self-assembled structures in the solutions.

polymer chain tethered to an insoluble solid spherical particle.[5] In his theory, the resulting aggregates can be pictured as a molten spherical core surrounded by the swollen tails. He referred to the resulting aggregates as bunchy micelles. One of the features of the bunchy micelles is the porous structure in the micellar core. In the macromolecules used in our research, there is a long PS chain tethered to a single-chain nanoparticle, and a polymer with such a structure can be used as a typical model to study the formation of bunchy micelles in a selective solvent. The self-assembly of the macromolecules was investigated in cyclohexane at a temperature above 35 °C. At this temperature cyclohexane is a good solvent for PS and a precipitant for PDMAEMA. A TEM image of aggregates of $NP_{0.1}$-$PDMAEMA_{74}$-*b*-$PS_{297}$ prepared from cyclohexane solution is shown in Figure 5a. In the image spherical aggregates with sizes in the range from 30 to 50 nm are observed. A magnified TEM image is shown in the insert of Figure 5a, from which it can be found that the core of the aggregate is composed of single-chain nanoparticles. The size distribution of the aggregates is also presented in the insert of Figure 5a. The bunchy micelles possess unimodal size distribution with hydrodynamic diameters in the range from 20 to 80 nm. The average hydrodynamic diameter of the bunchy micelles is about 33 nm. Our experimental results agree well with the theory


dx.doi.org/10.1021/mz300636x | *ACS Macro Lett.* 2013, 2, 100−106

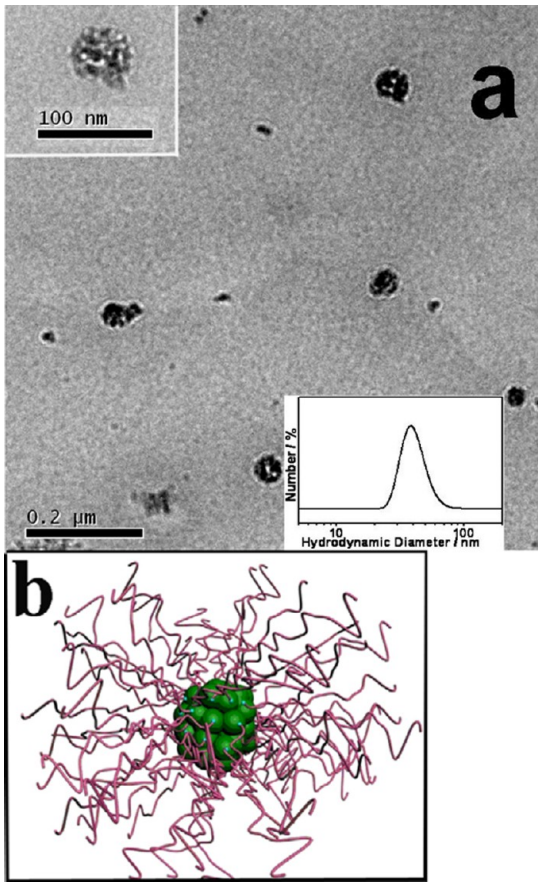


**Figure 5.** (a) A TEM image of self-assembly aggregates of $NP_{0.1}$-$PDMAEMA_{74}$-*b*-$PS_{297}$ in cyclohexane solution; (b) A cartoon picture showing structure of a bunchy micelle with single-chain nanoparticles in the core and soluble polymer tails in the corona.

proposed by Marques. In cyclohexane the shape amphiphile macromolecules self-assemble into bunchy micelles with positively charged single-chain nanoparticles in the cores and solvated PS in the coronae to stabilize the structures. The structure of the bunchy micelles is illustrated in Figure 5b.

In conclusion, we have demonstrated that PS tethered PDMAEMA single-chain nanoparticles can be used as building blocks in the fabrication of ordered structures. Depending on the PDMAEMA block length and the size of the single-chain nanoparticles, the shape amphiphiles can self-assemble into micellar or vesicular structures in aqueous and methanol solutions. In cyclohexane, the shape amphiphiles self-assemble into aggregates with single-chain nanoparticles in the cores and linear PS in the coronae. In the future, we hope to synthesize single-chain nanoparticles with controllable internal structures and create self-assembled structures with multifunctionalities.

## ■ ASSOCIATED CONTENT

### Supporting Information

Experimental part and a table showing the molecular weights and distributions of PS tethered single-chain nanoparticles and their precursors. This material is available free of charge via the Internet at http://pubs.acs.org.

## ■ AUTHOR INFORMATION

### Corresponding Author

*E-mail: nkliul@nankai.edu.cn; hyzhao@nankai.edu.cn.

### Notes

The authors declare no competing financial interest.

## ■ ACKNOWLEDGMENTS

This project was supported by the National Natural Science Foundation of China (NSFC) under Contract 21074058, and the National Basic Research Program of China (973 Program, 2012CB821500).

## ■ REFERENCES

(1) (a) Azzam, T.; Eisenberg, A. *Angew. Chem., Int. Ed.* **2006**, *45*, 7443−7447. (b) Balsara, N. P.; Tirrell, M.; Lodge, T. P. *Macromolecules* **1991**, *24*, 1975−1986. (c) Discher, D. E.; Eisenberg, A. *Science* **2002**, *297*, 967−973. (d) Riess, G. *Prog. Polym. Sci.* **2003**, *28*, 1107−1170.

(2) (a) Schacher, F. H.; Rupar, P. A.; Manners, I. *Angew. Chem., Int. Ed.* **2012**, *51*, 7898−7921. (b) Kim, S. H.; Nederberg, F.; Jakobs, R.; Tan, J. P. K.; Fukushima, K.; Nelson, A.; Meijer, E. W.; Yang, Y. Y.; Hedrick, J. L. *Angew. Chem., Int. Ed.* **2009**, *48*, 4508−4512.

(3) Glotzer, S. C. *Science* **2004**, *306*, 419−420.

(4) (a) Zhang, Z.; Horsch, M. A.; Lamm, M. H.; Glotzer, S. C. *Nano Lett.* **2003**, *3*, 1341−1346. (b) Glotzer, S. C.; Horsch, M. A.; Iacovella, C. R.; Zhang, Z.; Chan, E. R.; Zhang, X. *Curr. Opin. Colloid Interface Sci.* **2005**, *10*, 287−295. (c) Coluzza, I. ; van Oostrum, P. J. ; Capone, B. ; Reimhult, E.; Dellago, C. *Soft Matter* **2012**, DOI: 10.1039/c2sm26967h.

(5) Marques, C. M. *Langmuir* **1997**, *13*, 1430−1433.

(6) Han, Y.; Xiao, Y.; Zhang, Z.; Liu, B.; Zheng, P.; He, S.; Wang, W. *Macromolecules* **2009**, *42*, 6543−6548.

(7) (a) Yu, X.; Zhong, S.; Li, X.; Tu, Y.; Yang, S.; Horn, R. M. V.; Ni, C.; Pochan, D. J.; Quirk, R. P.; Wesdemiotis, C.; Zhang, W.; Cheng, S. Z. D. *J. Am. Chem. Soc.* **2010**, *132*, 16741−16744. (b) Yue, K.; Liu, C.; Guo, K.; Yu, X.; Huang, M.; Li, Y.; Wesdemiotis, C.; Cheng, S. Z. D.; Zhang, W. *Macromolecules* **2012**, *45*, 8126−8134.

(8) (a) Beck, J. B.; Killops, K. L.; Kang, T.; Sivanandan, K.; Bayles, A.; Mackay, M. E.; Wooley, K. L.; Hawker, C. J. *Macromolecules* **2009**, *42*, 5629−5635. (b) Murray, B. S.; Fulton, D. A. *Macromolecules* **2011**, *44*, 7242−7252. (c) Cherian, A. E.; Sun, F. C.; Sheiko, S. S.; Coates, G. W. *J. Am. Chem. Soc.* **2007**, *129*, 11350−11351. (d) Terashima, T.; Mes, T. T.; De Greef, F. A.; Gillissen, A. A. J.; Besenius, P.; Palmans, A. R. A.; Meijer, E. W. *J. Am. Chem. Soc.* **2011**, *133*, 4742−4745. (e) Foster, E. J.; Berda, E. B.; Meijer, E. W. *J. Am. Chem. Soc.* **2009**, *131*, 6964−6966.

(9) (a) Mecerreyes, D.; Lee, V.; Hawker, C. J.; Hedrick, J. L.; Wursch, A.; Volksen, W.; Magbitang, T.; Huang, E.; Miller, R. D. *Adv. Mater.* **2001**, *13*, 204−208. (b) Harth, E.; Horn, B. V.; Lee, V. Y.; Germack, D. S.; Gonzales, C. P.; Miller, R. D.; Hawker, C. J. *J. Am. Chem. Soc.* **2002**, *124*, 8653−8660. (c) Cherian, A. E.; Sun, F. C.; Sheiko, S. S.; Coates, G. W. *J. Am. Chem. Soc.* **2007**, *129*, 11350−11351. (d) Pyun, J.; Tang, C.; Kowalewski, T.; Fréchet, J. M. T.; Hawker, C. J. *Macromolecules* **2005**, *38*, 2674−2685. (e) Jiang, J.; Thayumanavan, S. *Macromolecules* **2005**, *38*, 5886−5891.

(10) (a) Cheng, C.; Qi, K.; Khoshdel, E.; Wooley, K. L. *J. Am. Chem. Soc.* **2006**, *128*, 6808−6809. (b) Cheng, C.; Qi, K.; Germack, D. S.; Khoshdel, E.; Wooley, K. L. *Adv. Mater.* **2007**, *19*, 2803−2835.

(11) Yuan, J.; Xu, Y.; Walther, A.; Bolisetty, S.; Schumacher, M.; Schmalz, H.; Ballauff, M.; Müller, A. H. E *Nat. Mater.* **2008**, *7*, 718−722.

(12) Bütün, V.; Lowe, A. B.; Billingham, N. C.; Armes, S. P. *J. Am. Chem. Soc.* **1999**, *121*, 4288−4289.

(13) Pomposo, J. A.; Perez-Baena, I.; Buruaga, L.; Alegría, A.; Moreno, A. J.; Colmenero, J. *Macromolecules* **2011**, *44*, 8644−8649.

(14) Ormategui, N.; García, I.; Padro, D.; Cabañero, G.; Grande, H. J.; Loinaz, I. *Soft Matter* **2012**, *8*, 734−740.

(15) Liu, S.; Weaver, J. V. M; Tang, Y.; Billingham, N. C.; Armes, S. P. *Macromolecules* **2002**, *35*, 6121−6131.

(16) Zhang, L.; Eisenberg, A. *Science* **1995**, *268*, 1728−1731.

(17) (a) Zhang, L.; Eisenberg, A. *Polym. Adv. Technol.* **1998**, *9*, 677–699. (b) Zhang, L.; Eisenberg, A. *Macromolecules* **1999**, *32*, 2239–2249.